


Article

Effect of Near-Freezing Temperature Storage on the Quality and Organic Acid Metabolism of Apple Fruit

Chang Shu ¹ , Bangdi Liu ^{2,3}, Handong Zhao ⁴, Kuanbo Cui ⁵ and Weibo Jiang ^{1,*}

¹ College of Food Science and Nutritional Engineering, China Agricultural University, Beijing 100083, China; sinosc@126.com

² Academy of Agricultural Planning and Engineering, Ministry of Agriculture and Rural Affairs, Beijing 100125, China; bangdi.liu@foxmail.com

³ Key Laboratory of Agro-Products Primary Processing, Ministry of Agriculture and Rural Affairs of China, Beijing 100125, China

⁴ School of Food Science and Engineering, Qilu University of Technology, Jinan 250353, China; qlspzhd@163.com

⁵ Agricultural Mechanization Institute, Xinjiang Academy of Agricultural Sciences, Urumqi 830091, China; widewave@126.com

* Correspondence: jwb@cau.edu.cn

Abstract: Organic acids play critical roles in fruit physiological metabolism and sensory quality. However, the conventional storage of apple fruit at 0 ± 0.1 °C cannot maintain fruit acidity efficiently. This study investigated near-freezing temperature (NFT) storage for ‘Golden Delicious’ apples, and the quality parameters, organic acid content, and malate metabolism were studied. The results indicate that NFT storage at -1.7 ± 0.1 °C effectively maintained the postharvest quality of apple fruit when compared to traditional storage at 0 ± 0.1 °C. Fruit that underwent NFT storage showed a better appearance and lower respiratory rate, ethylene production, weight loss, and malondialdehyde (MDA) content but higher firmness and soluble solids content. Further, fruit after NFT storage contained higher titratable acid (18.75%), malate (51.61%), citrate (36.59%), and succinate (2.12%) content when compared to the control after 250 days. This was achieved by maintaining higher cytosolic NAD-dependent malate dehydrogenase (cyNAD-MDH), phosphoenolpyruvate carboxylase (PEPC), vacuolar H⁺-ATPase (V-ATPase), and vacuolar inorganic pyrophosphatase (V-PPase) activities that promote malate biosynthesis and accumulation while inhibiting enzyme activity that is responsible for malate decomposition, including phosphoenolpyruvate carboxylase kinase (PEPCK) as well as the cytosolic NAD phosphate-dependent malic enzyme (cyNADP-ME). Further, storage at NFTs maintained a higher expression of malate biosynthesis-related genes (*MdcyNAD-MDH* and *MdPEPC*) and transport-related genes (*MdVHA* and *MdVHP*) while suppressing malate consumption-related genes (*MdcyME* and *MdPEPCK*). The results demonstrate that NFT storage could be an effective application for apple fruit, which maintains postharvest quality and alleviates organic acid degradation.

Keywords: *Malus domestica* Borkh.; ice temperature; postharvest quality; malate metabolism



Citation: Shu, C.; Liu, B.; Zhao, H.; Cui, K.; Jiang, W. Effect of Near-Freezing Temperature Storage on the Quality and Organic Acid Metabolism of Apple Fruit. *Agriculture* **2024**, *14*, 1057. <https://doi.org/10.3390/agriculture14071057>

Academic Editor: Isabel Lara

Received: 5 June 2024

Revised: 27 June 2024

Accepted: 28 June 2024

Published: 30 June 2024



Copyright: © 2024 by the authors. Licensee MDPI, Basel, Switzerland. This article is an open access article distributed under the terms and conditions of the Creative Commons Attribution (CC BY) license (<https://creativecommons.org/licenses/by/4.0/>).

1. Introduction

Apples are one of the most important fruit crops. They are produced in high volumes and utilized in numerous processed products. Apple fruit also contain bioactive compounds beneficial to human health [1]. Like other climacteric fruit, apples exhibit an increased respiratory rate during maturation and storage [2]. Apple senescence is followed by quality decrease comprising texture mealiness, flavor and color deterioration, and weight loss. Controlled atmosphere storage (CA) and postharvest treatments, such as 1-methylcyclopropene (1-MCP), novel edible coating [3], cold plasma [4], and electrolyzed water treatment [5], can significantly prolong apple availability; however, these methods may also increase the potential risks to fruit during storage, such as physiological disorders and ripening interruption [6]. Physical treatments have attracted research interest in

controlling quality deterioration as well as postharvest diseases in fresh produce, with the benefits of easy application and reliability, no risk of residue in the treated product, and low environmental impact [7]. Consequently, efficient and convenient methods need to be developed to slow senescence and thereby reduce the quality loss of postharvest apples.

As a controlled freezing storage technology, near-freezing temperature (NFT) storage lowers the storage temperature below 0 °C while stabilizing it above the biological freezing temperature of tissues [8]. By precisely controlling storage temperature fluctuations, storage temperatures are minimized, and the metabolic processes and enzyme activities responsible for deterioration are inhibited, therefore extending the storage life. Some studies utilized physical and chemical methods to adjust the biological freezing point, which can further reduce the storage temperature to inhibit physiological processes [9]. Postharvest apricot [10], avocado [11], blueberry [9], guava [12], nectarine [13], sweet cherry [14], and green beans [15] were successfully stored at NFTs, with good preservation of physiological and commercially desirable qualities. However, there has been insufficient investigation into the impact of NFT storage on apple quality.

Organic acids play multiple physiological roles in energy substance generation, the storage of carbon, and amino acid biosynthesis [16]. They also contribute to fruit acidity, together with soluble sugar, volatiles, etc., determining fruit acidity and overall acceptability [17]. Fruit acidity has also been defined as an essential quality parameter for further processing [18]. Previous research has assessed the impact of storage temperature on the levels of organic acids and the metabolic processes of apple and other fruit. They have demonstrated that lower temperatures contribute to the maintenance of organic acids, while higher temperatures facilitate their decomposition [19,20]. Meanwhile, higher expressions of organic acid decomposition-related genes were positively correlated with higher storage temperatures [21,22]. The organic acid content contributes to fruit quality, prolongs shelf-life, and provides resistance against stresses [23]. Thus, understanding how postharvest storage influences fruit acidity is vital for improving postharvest fruit quality.

Although fruit contain a variety of organic acid components, such as citric, tartaric, succinic, and malic acid, the acidity of fruit is mostly determined by the presence of one or two of these acids. In apple cells, around 90% of the total organic acids are malic acid, with a concentration of 1.72 to 29.27 mg g⁻¹, and other organic acid components, such as citric acid, are present in small amounts that contribute less to the apples' acceptability [24]. Malate, including its salt and ester form, is the major physiological form in cells. The malate content is dependent on the dynamic metabolic balance between its synthesis, degradation, and transportation [25]. The malate content in apple fruit gradually increases during the growth of the fruit and thereafter decreases consistently throughout fruit ripening and storage [26]. Two enzymes respond to malate's generation: cyNAD-MDH converts oxaloacetate (OAA) into malic acid in the cytoplasm [25,27], and PEPC converts phosphoenolpyruvate (PEP) to malic acid as part of the mitochondrial tricarboxylic acid cycle [28]. The generated malic acid primary storage by vacuoles is determined by tonoplast transporters and proton pumps (V-ATPase and V-PPase) that generate the electrochemical gradient for malate transport into the vacuoles [16,29]. The stored malate is degraded or metabolized by cyNADP-ME and PEPCK [24,30]. These key enzymes participate in various physiological metabolisms of cells and malate, and their combined effect determines the intracellular malate concentration. Recent studies reveal the regulation of malate metabolism by postharvest treatments [22,31,32], and further research reveals the molecular mechanisms of this process [33].

Previous studies have demonstrated that NFT storage maintains the postharvest quality and acidity of apricot [17] and sweet cherry [14] fruit. However, no research has investigated apple storage using NFTs, and reports on organic acid metabolism in fruit storage at NFTs are limited. This study examined the effect of NFT storage on the quality and malate metabolism of apples, and the quality attributes, organic acid content, and expression and activity of enzymes responsible for malate metabolism were studied in

detail. This research may provide some theoretical basis for how NFT storage regulates fruit malate metabolism.

2. Materials and Methods

2.1. Plant Materials and Experiment Design

'Golden Delicious' apples (1770 fruit per independent validation) were harvested from an orchard in the Haidian district, Beijing, China, in 2018. The experiment conducted three independent validations. The fruit were at the commercial maturity stage (135 to 140 days from full bloom), of uniform size (150 ± 20 g) and color ($L^* = 65.03 \pm 2.62$, $a^* = -10.0 \pm 0.80$, $b^* = 29.60 \pm 1.52$), and without visual defects or mechanical injury. The initial fruit quality parameters were as follows: their firmness was 79.52 ± 2.22 N, the SSC was $13.7 \pm 0.36\%$, and the TA was $0.63 \pm 0.02\%$. They were packed in shipping boxes (about 45 fruit in each box) and transported to the postharvest lab of China Agricultural University within 2 h. The fruit were washed with sodium hypochlorite (2%, v/v) for 2 min, rinsed with water, and left to dry at room temperature. Then, they were pre-cooled at $5 \text{ }^\circ\text{C} \pm 0.1 \text{ }^\circ\text{C}$ for 24 h, randomly separated into two groups, and stored at $0 \text{ }^\circ\text{C} \pm 0.1 \text{ }^\circ\text{C}$ (control) and NFTs ($-1.7 \text{ }^\circ\text{C} \pm 0.1 \text{ }^\circ\text{C}$). The 3 replicates equated to 6 lots, with 150 fruit per lot. An extra 360 fruit for each group were randomly collected for consumer tests after the storage period. The temperature for NFT storage was determined to be $-1.7 \pm 0.1 \text{ }^\circ\text{C}$, which is slightly higher than that of the supercooling point temperature ($-2.0 \text{ }^\circ\text{C}$) referred to in our previous method [13], which is shown in the Supplemental Material (Figure S2). The fruit were stored in a modified storage system (Youbuni, Beijing, China) for 250 days (Figures S1 and S2A,B). The fruit were packed in plastic baskets and sealed in polyethylene bags (<0.04 mm), with 85–95% relative humidity. Twenty fruit per group were collected at 50-day intervals for biological analysis. Flesh tissue was excised from the equatorial area of each fruit, cut into small pieces, wrapped in aluminum foil, and finally kept in a freezer at $-80 \text{ }^\circ\text{C}$. Over the storage period, the freezing point of fruit increases in response to changes in the soluble solids content. To avoid freezing damage that may cause an extremely high risk of total loss, the storage temperature of the NFT group was adjusted every 50 days. The NFTs during storage are shown in Table S1. Fruit soluble solids and the NFTs show a good correlation: the mathematical model is $Y = -0.218X + 1.33$, $R^2 = 0.936$ (Table S1 and Figure S3), where Y is the NFT, and X is the soluble solids content. Each group contained three replications, and all experiments were performed in triplicate.

2.2. Measurement of Fruit Quality Parameters

A fruit texture analyzer (GY-1, Tuopu Instrument Co., Ltd., Tianjin, China) was used to measure pulp firmness. The diameter of its probe was 3.5 mm, and the readings were calculated as Newtons. Fruit juice (20 mL) was read by a digital sugar meter (PAL-1, Atago, Tokyo, Japan), and the results are in percent (%). Peel color was measured by a spectrophotometer (NF333, Nippon Denshoku Industries, Tokyo, Japan). The probes were placed on four opposite positions along the equatorial peel, and the L^* , a^* , and b^* values were measured. Weight loss was calculated as the mass change when compared with the fruit weight at day 0. To avoid the effects of low surface temperature and condensation on the determination, all the fruit selected for quality parameters were moved to room temperature conditions until their core temperature returned to $25 \text{ }^\circ\text{C}$ before parameter measurement.

The concentration of malondialdehyde (MDA) was assayed by the thiobarbituric acid method, and the results were calculated as $\mu\text{mol kg}^{-1}$ on a fresh weight basis [14]. Membrane permeability was assessed using the relative electrical conductivity method [34], and the results are expressed as relative conductivity (%).

2.3. Respiratory Rate and Ethylene Production Determination

Fruit respiration intensity and ethylene production rate were determined according to a prior method [17]. The fruit were left to warm to room temperature and then sealed

in a cabinet (2.3 L), and all the operations were under room temperature. After two hours, the internal gas was fully mixed with a syringe, and 1.0 ml of headspace gas was taken for measurement. A gas chromatograph system (GC-7890F, Shanghai Techcomp Bio-equipment, Shanghai, China) was used to measure the respiratory rate ($\mu\text{mol kg}^{-1} \text{s}^{-1}$ of CO_2) and ethylene production ($\text{kg}^{-1} \text{s}^{-1}$ of C_2H_4) of the fruit.

2.4. Consumer Tests

A sensory test was performed after 250 days of storage (refer to a previous procedure [35]). A taste panel containing 12 participants from China Agricultural University was trained [36] and responsible for each group tested, with each consumer evaluating three randomly selected apples for their general acceptability (1 = extremely dislike, 5 = in the middle of like/dislike, and 9 = extremely like). Visual appearance, sweetness, sourness, and juiciness were evaluated to characterize apple acceptability. The whole test was performed at 23 to 25 °C, and the lab was equipped with individual booths for the testers. The samples were at room temperature and presented using uniform food containers in random order.

2.5. Assayment of Organic Acid Content

Organic acid extraction and determination were based on the report proposed by previous research [35,37], with some modifications. Briefly, 3.0 g of frozen flesh tissue was homogenized in 10 mL of deionized water and then shaken at 25 °C for one hour. The mixture was centrifugated, and the supernatant was taken and filtered with a water syringe filter (0.22 μm) before analysis.

Titrateable acid (TA) was measured by titrating the juice with NaOH standard solution (0.1 mol L^{-1}), and the result was calculated as the percent of malic acid in fresh weight (%). The individual organic acids were analyzed by an ion chromatography system (ICS-1100, Thermo Fisher, Waltham, MA, USA). A sample (25 μL) was injected into the IC system, and KOH solution was used as the mobile phase flowing at 1 mL min^{-1} . The elution gradient was as follows: 0 to 20 minutes was 3 mmol L^{-1} , and 20 to 120 min was 3–40 mmol L^{-1} . The IC system consisted of a column (IonPac AS23), a conductivity detector, and a suppressor (AERS 500). The detector was operated at 35 °C, and the column ran under 30 °C. The data were processed by Chromeleon 7.1 software, and the individual organic acid components were quantified by comparing the retention time and peak area between the samples and organic acid standards. All the standards were obtained from Sigma-Aldrich (St. Louis, MO, USA). The results were calculated as g per kg of fresh weight.

2.6. Malate Metabolism-Related Enzyme Activity Determination

The enzymes were extracted and purified referring to previous methods [26,31,38]. Ten grams of frozen tissue was ground with an extract solution at 4 °C. The extract solution contained HEPES-Tris (50 mmol L^{-1} , pH 7.6), 250 mmol L^{-1} of sorbitol, 125 mmol L^{-1} of KCl, 5 mmol L^{-1} of ethylene glycol bis (β -aminoethyl ether)- N,N,N',N' -tetraacetic acid (EGTA), 10 mmol L^{-1} of MgSO_4 , 2 mmol L^{-1} of phenylmethane sulfonyl fluoride (PMSF), 1.5% (w/v) polyvinylpyrrolidone (PVP), 0.1% (w/v) bovine serum albumin (BSA), and 1 mmol L^{-1} of dithiothreitol (DTT). The mixture was centrifuged at $1000 \times g$ for 15 min to remove fruit residue and cell debris. The supernatant was centrifuged again at $50,000 \times g$ for 1 h, and then the supernatant was further passed through Sephadex G-25 gel for desalting. The extracts were used for measuring enzyme activities. The precipitate (tonoplast vesicles) was further purified by the density gradient centrifugation method [30]. A 0%/30% (w/v) discontinuous sucrose gradient was used as the dielectric gradient. After centrifuging at $100,000 \times g$ for 2 h, the interphase was collected and utilized to assay V-ATPase and V-PPase activities.

The activity of cyNAD-MDH was measured as previously described [29], with some modifications. A reaction system of 1 mL volume containing 50 mmol L^{-1} of Tris-HCl (pH 7.8), 2 mmol L^{-1} of MgCl_2 , 0.5 mol L^{-1} of EDTA, 0.2 mmol L^{-1} of NADH, and 50 μL of the enzyme extract was set. The reaction was activated by 2 mmol L^{-1} of oxaloacetate.

The activity of cyNADP-ME was determined according to the procedures described by Han et al. [32]. The reaction mixture consisted of 80 mmol L⁻¹ of Tris-HCl (pH 7.5), 0.1 mmol L⁻¹ of EDTA, 1.0 mmol L⁻¹ of DTT, 0.2 mmol L⁻¹ of NADP, 0.4 mmol L⁻¹ of MnSO₄, and 200 µL of crude enzyme extract. The reaction was initiated by adding L-malate to a final concentration of 10 mmol L⁻¹. The activity of PEPC was assayed according to the procedure described by Liu et al. [31], with slight modifications. The reaction mixture (1 mL) consisted of 50 mmol L⁻¹ of Tris-HCl (pH 8.0), 2 mmol L⁻¹ of DTT, 5 mmol L⁻¹ of MgCl₂, 0.2 mmol L⁻¹ of NADH, 10 mmol L⁻¹ of NaHCO₃, 5 U of NAD-MDH, and 50 µL of enzyme extract. The reaction was activated by adding phosphoenolpyruvate (PEP) to a final concentration of 2.5 mmol L⁻¹. The assay for PEPCK activity was based on a previous method [39], with some modifications. The reaction system contained 100 mmol L⁻¹ of HEPES-KOH (pH 6.8), 100 mmol L⁻¹ of KCl, 0.14 mmol L⁻¹ of NADH, 6 mmol L⁻¹ of MnCl₂, 2 mmol L⁻¹ of DTT, 6 mmol L⁻¹ of PEP, 1.0 mmol L⁻¹ of adenosine diphosphate (ADP), 90 mmol L⁻¹ of KHCO₃, 6 U of NAD-MDH, and 100 µL of enzyme extract. The reaction was activated by adding PEP to a final concentration of 6 mmol L⁻¹. Absorbance was measured at 340 nm, and all enzyme activities were expressed in U mg⁻¹ protein. One unit of enzyme activity was defined as the amount of enzyme that could oxidize 1 mM of NADH (or NADPH) per min at 25 °C.

The activities of V-ATPase and V-PPase were assayed according to the procedure described by Liu et al. [38], with some modifications. Enzyme activities were determined by measuring the quantity of inorganic phosphorus released from the reaction solution. The 1 mL reaction volume contained 30 mmol L⁻¹ of HEPES-Tris (pH 7.0 for V-ATPase and pH 8.5 for V-PPase), 3 mmol L⁻¹ of MgSO₄, 50 mmol L⁻¹ of KCl, 0.5 mmol L⁻¹ of NaN₃, 0.2 mmol L⁻¹ of Na₃VO₄, 0.2 mmol L⁻¹ of ammonium molybdate, and 30 µL of tonoplast vesicles. ATP-Na₂ (a final concentration of 3 mM for V-ATPase) or Na₄P₂O₇ (a final concentration of 2 mM for V-PPase) was added to activate the reaction. The reaction was performed at 37 °C for 30 min, and 50 µL of trichloroacetic acid (TCA) was added to terminate the reaction. The released inorganic phosphate was measured according to a previous method [40]. The enzyme activity was calculated by the rate of 1 µmol of phosphorus released every minute detected at 660 nm and finally expressed as U mg⁻¹ of protein. The protein content was measured using the Bradford test [41], and bovine serum albumin (BSA) served as the standard for quantification.

2.7. Real-Time Quantitative PCR

Fruit total RNA extraction and cDNA transcription were performed following the instructions of the manufacturer (TransGen Biotech Co., Ltd., Beijing, China). The sequences of the primers used are shown in Table 1.

Table 1. Primer sequences used for quantitative real-time PCR.

Gene	Forward Primer (5'-3')	Reverse Primer (5'-3')
<i>MdActin</i>	CTCCCAGGGCTGTGTTTCCTA	GGCATCCTTCTGACCCATACC
<i>MdcyMDH</i>	AGCCGCAGGACAAATTGGAT	GTTGACTCCAGTGCATGCCTC
<i>MdcyME</i>	GCTGAAAGCTGTATGTACAGCCC	CTCCTAACCCAGCTACCTGC
<i>MdPEPC</i>	CAAGCCGGCTAATGAACTTG	GGCATCATCCACTTTCGGGT
<i>MdPEPCK</i>	GTCAGGTAAGGAAAGACGACTC	CCAACGCATGGTATCTTTGC
<i>MdVHA-A</i>	TGGCTGAAATGCCTGCAGAT	TTTACCCGCCCGTTCGTAA
<i>MdVHP</i>	CTGGTGCTGCAACGAACGT	AAACGCAATGGCGAACACA

The reference gene, *MdActin*, was chosen, and the 2^{-ΔΔC_t} methodology was used to determine the relative transcription level [42]. The determination includes 3 biological replicates, and each sample was performed 3 individual times.

2.8. Data Analysis

The experiments were performed in triplicate and repeated three times, and statistical analysis was performed using SPSS software version 20.0 (SPSS-IBM Inc., Armonk, NY, USA) and visualized by Origin 9.0 software. All the results are shown as means \pm standard error. One-way analysis of variance (ANOVA) was used to compare various groups at each time point. Differences were regarded as significant when the p -value was below 0.05, as determined using Duncan's multiple-range test.

3. Result and Discussion

3.1. Effects of NFT Storage on Fruit Quality

Storage at NFTs retained the appearance of the fruit: the fruit surfaces were relatively plump after NFT storage, and the stems were still sturdy and green (Figure 1). The increased a^* and b^* values represent the faded green color and increased yellowing of the peel, respectively. This trend was significantly suppressed during storage at NFTs. At the end of storage, the b^* value of the fruit stored at NFTs was 16.07% lower ($p < 0.05$) than the control group. Storage at NFTs inhibited the green-to-yellow peel color change. In the control group, the L^* value first rose and subsequently declined after day 150, while it continuously increased in the NFT storage group. This suggests that the peel color darkened during prolonged storage under the control conditions, whereas it brightened during storage at NFTs.

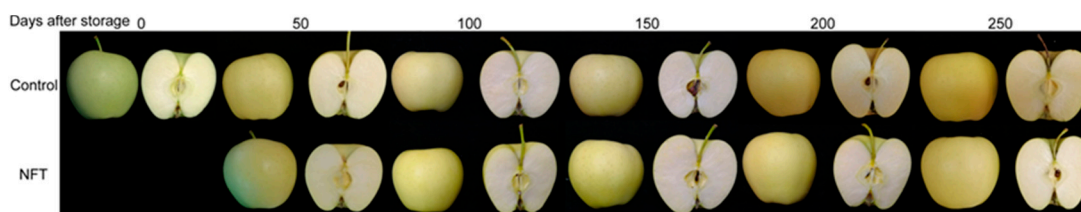


Figure 1. Effect of NFT storage on fruit appearance.

The sensory attributes of apples were analyzed by descriptive analyses. The evaluation parameters included visual appearance, sweetness, sourness, juiciness, and consumer satisfaction (Figure 2D). The total consumer satisfaction for apples that had undergone NFT storage was higher than that of the control. Notably, the biggest gap was recorded in the sourness scores between the control and NFT storage groups. These findings suggest that storing the fruit at NFTs enabled them to maintain their sensory characteristics and delayed the decrease in fruit acidity.

The respiratory rate of the control fruit increased at a higher level during storage, with the highest value recorded on day 50, and decreased after 150 days of storage. However, the apples from the NFT treatment showed an increased respiratory rate but did not show an obvious peak value (Figure 3A). Storage at NFTs slowed the respiratory rate and significantly ($p < 0.05$) suppressed the peak value. The firmness of pulp was significantly reduced throughout the storage period in the control group (Figure 3C); however, the decline in flesh firmness was delayed upon storage at NFTs. The flesh firmness of NFT-stored apples was 23.45% ($p < 0.05$) higher than that of apples stored under the control conditions at day 250. Storage at NFTs also resulted in the maintenance of the SSC, which was higher than that of the control during the storage period (Figure 3D). Apples stored at NFTs exhibited significantly reduced weight loss (Figure 3E). The weight loss of apples stored at NFTs was 18.98% lower ($p < 0.05$) than the control. Membrane permeability (Figure 4) and the MDA (Figure 3F) content are indicators of plasma membrane integrity. Storage at NFTs effectively inhibited the loss of cell membrane integrity. These findings indicate that storing apples at NFTs efficiently preserved their quality and delayed their deterioration.

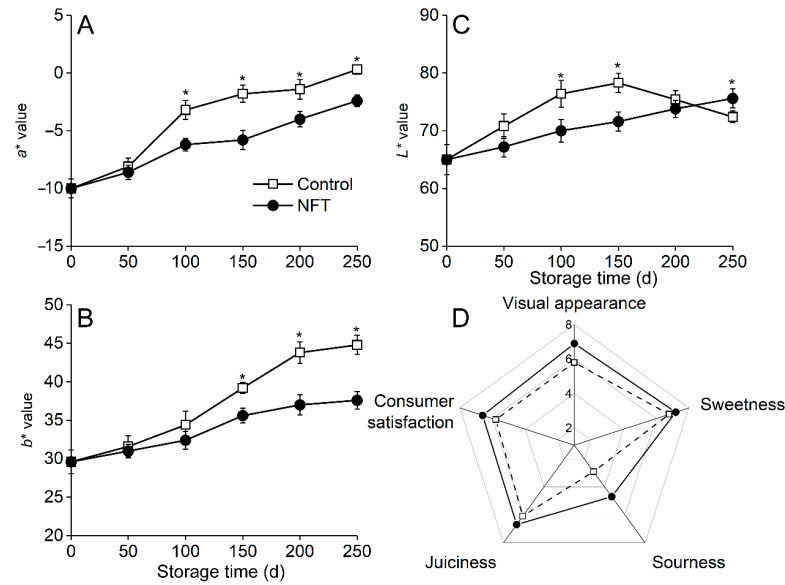


Figure 2. Effect of NFT storage on fruit peel: a^* (A), b^* (B), L^* (C) value changes during storage. Sensory evaluation after storage (D). Each value is the mean of three replicates for three independent experiments and expressed as mean \pm standard error ($n = 3$). Asterisks represent significant differences (one-way ANOVA, $p < 0.05$) according to Duncan's multiple-range test.

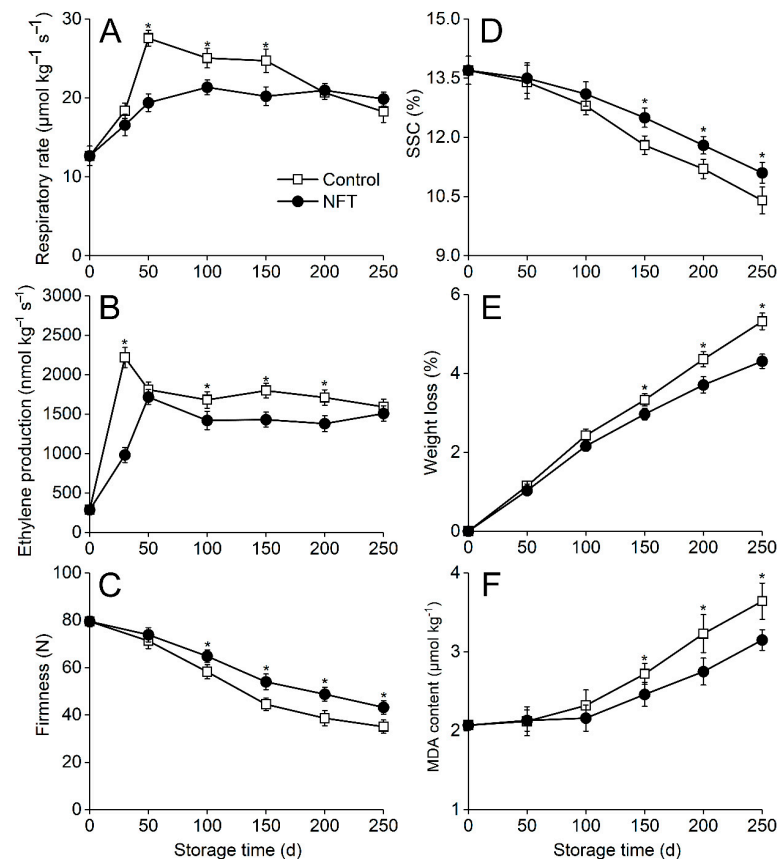


Figure 3. Respiratory rate, ethylene production, and postharvest quality of apple fruit under NFT storage. Respiratory rate (A), ethylene production (B), pulp firmness (C), soluble solids content (D), weight loss (E), and malondialdehyde content (F). Each value is the mean of three replicates for three independent experiments and expressed as mean \pm standard error ($n = 3$). Asterisks represent significant differences (one-way ANOVA, $p < 0.05$) according to Duncan's multiple-range test.

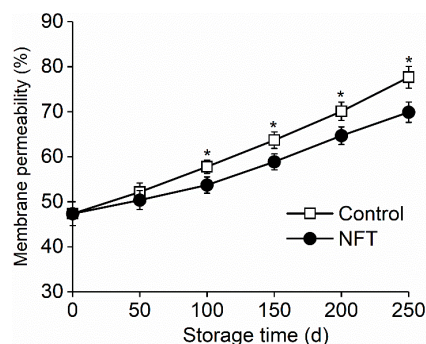


Figure 4. Effect of NFT storage on membrane permeability of apple fruit. Each value is the mean of three replicates for three independent experiments and expressed as mean \pm standard error ($n = 3$). Asterisks represent significant differences (one-way ANOVA, $p < 0.05$) according to Duncan's multiple-range test.

In this study, to avoid freezing injury, the storage temperature was set at -1.7 ± 0.1 °C, which is 0.3 °C higher than the supercooling point. A modified storage system was utilized to precisely control the temperature (Figure S1). Previous studies have reported the possible mechanisms by which NFT storage significantly suppresses fruit ripening. The liquid within fruit tissue gradually solidifies into a glassy state when the fruit is exposed to temperatures near the biological freezing point. In this state, the rate of molecular diffusion in the fruit is extremely low [43], leading to the inhibition of chemical reactions, such as respiratory metabolism, which require molecular diffusion [44]. This indicates that NFT storage markedly delays the postharvest ripening process of apples, including a decline in firmness, color change, and TA, compared to traditional storage at 0 °C. These observations in apples are in line with findings from recent studies on apricots, nectarines, and sweet cherries.

Commercial quality specifications for apples rely mainly on visual appearance and color. The peel color turns from green to yellow, a process that is regulated via chlorophyll degradation and carotenoid synthesis and results in increased a^* and b^* values and a decreased L^* value. However, our data suggest that the L^* value of apples stored at 0 °C increases consistently during the early period and then decreases during the last 50 days (Figure 2C). This may be associated with the change in the peel color process from green to bright green, finally turning yellow with brown spots [45]. Flesh firmness is considered one of the most important criteria of apple quality. The rapid softening of 'Golden Delicious' apples is associated with pectin depolymerization [46]. Storage at NFTs delayed the softening process (Figure 3B), and it possibly inhibited the activities of cell wall-modifying enzymes that regulate the softening process [15,47]. Membrane integrity was reflected in the MDA content and membrane permeability, which are indicators of fruit cell senescence. Storage at NFTs maintained a lower MDA content and membrane permeability and suppressed lipid peroxidation. These findings align with a previous study [14] reporting that NFT storage maintained fruit quality and higher antioxidant levels in sweet cherries. Consumer expectations for acceptable 'Golden Delicious' apple palatability include a minimum of 12% SSC, 3.2 mg g^{-1} malate content, and 44 N firmness [44], which may explain the higher consumer satisfaction with apples stored at NFTs.

3.2. Effects of NFT Storage on Fruit Organic Acid Content

TA in the control fruit declined continuously during storage (Figure 5A). Storage at NFTs significantly delayed the decline tendency of TA, with a level 18.75% higher ($p < 0.05$) than the control group at day 250. The content of malate, citrate, and succinate, which are the three primary organic acids in apples, was also evaluated (Figure 5B–D). Similar to the trend for TA, malate and citrate contents decreased gradually during storage. Storage at NFTs effectively inhibited this decline. There was no significant difference in the succinate content between the control and apples stored at NFTs over the storage period, except on

day 150. These results indicate that NFT storage alleviates the degradation of the organic acid content and results in higher titratable acid and individual organic acid contents, contributing to the maintenance of fruit acidity.

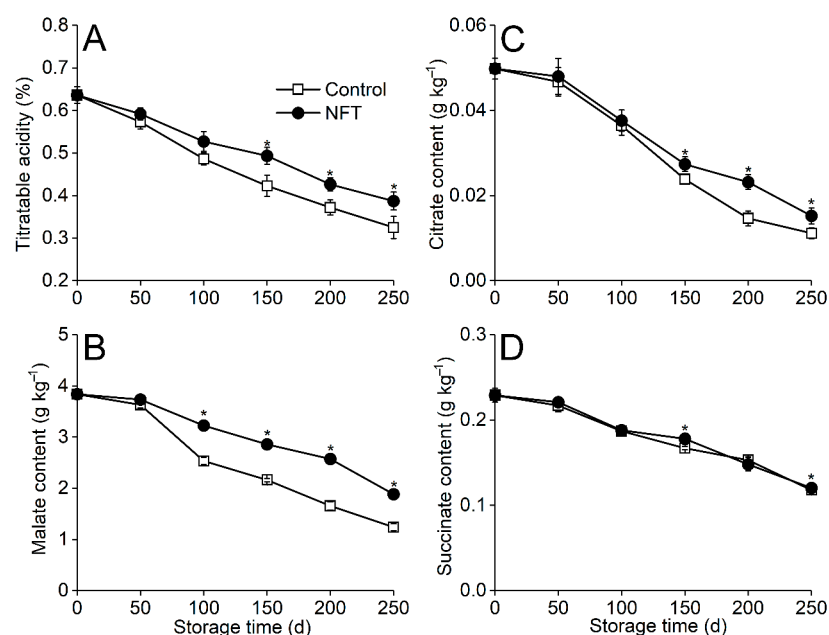


Figure 5. Changes in organic acid content in apple fruit during postharvest storage. Titratable acid (A), malate (B), citrate (C), and succinate (D) contents. Each value is the mean of three replicates for three independent experiments and expressed as mean \pm standard error ($n = 3$). Asterisks represent significant differences (one-way ANOVA, $p < 0.05$) according to Duncan's multiple-range test.

3.3. Effects of NFT Storage on the Activities of Enzymes Involved in Malate Metabolism

PEPC and cyNAD-MDH are crucial for malate synthesis. In the control group, the cyNAD-MDH activity peaked after 50 days of storage and then decreased rapidly and maintained lower levels compared to the NFT group (Figure 6A); however, this decline was significantly delayed ($p < 0.05$) upon storage at NFTs. PEPC activity reached a peak at day 50 and continuously declined to a level lower than the initial level on day 0 (Figure 6B). Apples stored at NFTs maintained a relatively high level of PEPC activity during subsequent storage. cyNADP-ME activity exhibited an initial increase during the first 50 days, followed by a subsequent decrease. Throughout storage, the NFT group consistently showed lower cyNADP-ME activities compared to the control (Figure 5C). The activity of PEPCK showed a moderate increase over storage in the control fruit; however, this trend was mitigated in the NFT-stored fruit, which exhibited reduced PEPCK activity compared to that of the control (Figure 6D). These results suggest that NFT storage suppressed the increased activities of malate decomposition-related enzymes.

V-ATPase and V-PPase are vacuolar pumps essential for the maintenance of malate homeostasis. In the control fruit, V-ATPase activity declined overall during storage, showing an initial increase and then declining gradually during subsequent storage; V-PPase activity increased in the initial stage and then declined gradually in the subsequent storage (Figure 4E,F). The activities of these enzymes were maintained at significantly higher levels in fruit stored at NFTs.

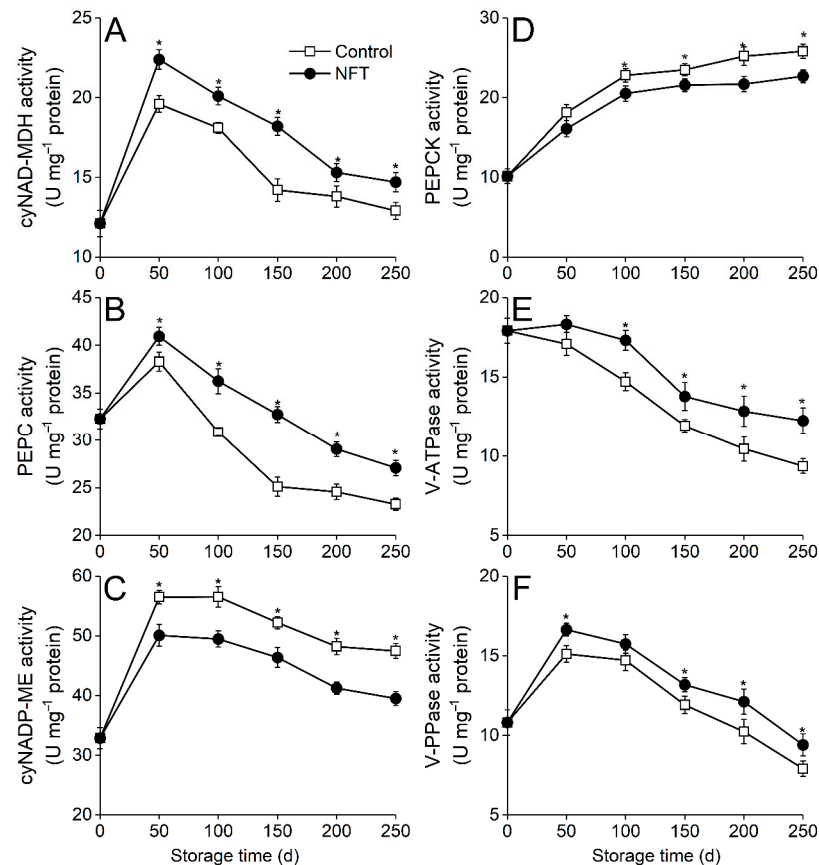


Figure 6. Effects of NFT storage on malate metabolism enzyme activity of apple fruit. Activities of cytosolic nicotinamide adenine dinucleotide-dependent malate dehydrogenase (cyNAD-MDH) (A), phosphoenolpyruvate carboxylase (PEPC) (B), cytosolic NAD phosphate-dependent malic enzyme (cyNADP-ME) (C), phosphoenolpyruvate carboxylase kinase (PEPCK) (D), H⁺-ATPase (V-ATPase) (E), and vacuolar inorganic pyrophosphatase (V-PPase) (F). Each value is the mean of three replicates for three independent experiments and expressed as mean \pm standard error ($n = 3$). Asterisks represent significant differences (one-way ANOVA, $p < 0.05$) according to Duncan's multiple-range test.

Malate biosynthesis is regulated by cyNAD-MDH and PEPC. Storage at NFTs maintained higher activities, as well as higher corresponding transcript levels of the malate synthesis-related enzymes. The expression of *MdcyMDH* and *MdPEPC* involved in malate synthesis was higher compared to those at the control temperature (Figures 6 and 7). This demonstrates that NFT storage enhances malate biosynthesis via the regulation of cyNAD-MDH and PEPC activities and the corresponding gene expression. Vacuolar pumps establish the electrochemical gradient across the tonoplast for the compartmentalization of organic acids [16]. The activity of the V-PPase enzyme, along with the consistent expression level of *MdVHP*, increased during the first 50 days and then decreased, which may be related to a compensatory response to the tonoplast proton flux [30]. Similarly, the V-ATPase activity and *MdVHA-A* transcript levels were both higher than those of the control. The present results demonstrate that NFT storage induces higher activities of the enzymes involved in malate biosynthesis and upregulates the corresponding transcript levels, indicating that NFT storage can result in the maintenance of a higher content of malate.

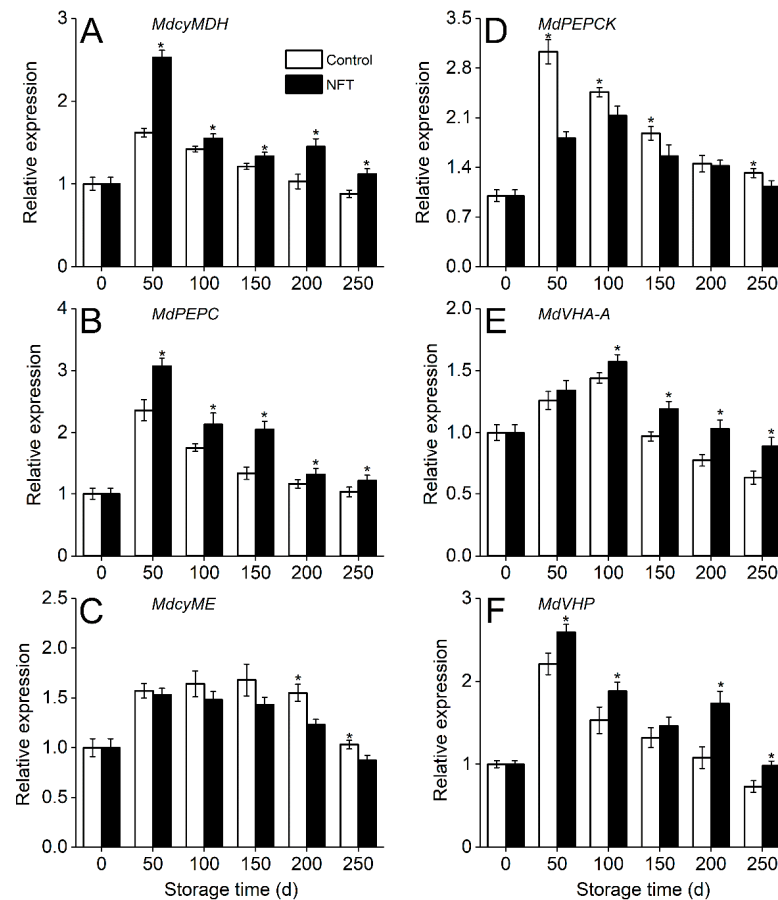


Figure 7. Effects of NFT storage on gene transcript levels involved in malate metabolism in apple fruit. Transcript levels of *MdcyNAD-MDH* (A), *MdPEPC* (B), *MdcyME* (C), *MdPEPCK* (D), *MdVHA-A* (E), and *MdVHP* (F). Each value is the mean of three replicates for three independent experiments and expressed as mean \pm standard error ($n = 3$). Asterisks represent significant differences (one-way ANOVA, $p < 0.05$) according to Duncan's multiple-range test.

3.4. Gene Expression Involved in Malate Metabolism

The relative expression levels of genes encoding enzymes involved in malate metabolism in apples were monitored. Apples subjected to NFT storage exerted higher *MdcyMDH*, *MdPEPC*, *MdVHP*, and *MdVHA-A* levels but lower *MdPEPCK* expression levels compared to those stored at the control temperature. The *MdcyME* transcript level showed only a marginal change upon storage at NFTs, except on day 200 (Figure 7). The results suggest that storing apple fruit at NFTs results in the increased expression of key genes involved in the synthesis of organic acids while decreasing the expression of genes involved in the decomposition of malate.

Correspondingly, enzyme activity related to malate degradation was downregulated by storage at NFTs. The activity of PEPCK was significantly inhibited upon NFT storage. As PEPCK is involved in gluconeogenesis, we conclude that either malate conversion to sugar or malate metabolized through gluconeogenesis may have been suppressed throughout NFT storage [46]. The activity of cyNADP-ME initially increased and then decreased consistently with prolonged storage and was downregulated by NFT storage. However, inconsistent patterns were observed between the gene transcript level and cyNADP-ME activity, and no difference was observed between the control and NFT-stored fruit, except at days 200 and 250. One of the possible explanations is the post-translational regulation of cytosolic pH values as well as the malic acid and/or malate content [26]. Similar results were observed for the *MdcyNADP-ME* expression levels in apples during storage in response to GABA treatment [32]. Follow-up studies need to further study shelf-life

after storage, the multiple forms of genes, the systemic interaction between multiple genes associated with malate metabolism, and the role of other transcription factors in response to storage/treatments [33].

3.5. Clustering and Correlation Analysis

Cluster analysis of the indicators measured in this study (Figure 8) found that compared with conventional cold storage, NFT storage significantly alleviated the decline in edible quality and inhibited physiological changes related to maturation and senescence. NFT storage also slowed the decline in the SSC and maintained the content of total titratable acid and various organic acids. The measurement of the key enzyme activities of malate metabolism and the corresponding gene expression found that NFTs can significantly maintain the biosynthesis of malate, reduce its biodegradation, and promote its transvacuole transport and storage by increasing the activity of vacuolar V-ATPase and V-PPase activity. These results indicate that NFT can effectively maintain 'Gloden Delicious' apple quality and maintain organic acid concentrations.

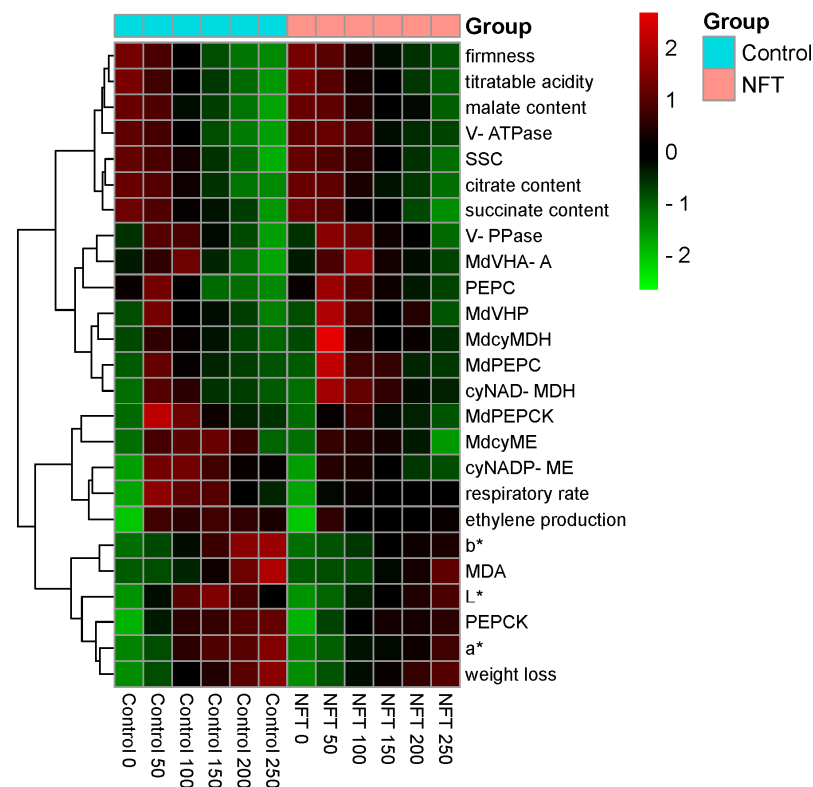


Figure 8. Cluster heatmap analysis among the measured parameters. The heatmap illustrates the relative intensity of different parameter changes subjected to different storage at 0 °C compared with NFTs.

The correlation heatmap (Figure 9) shows the indicators measured in the study are clustered into three categories. Peel color indicators, respiration, ethylene production intensity, and PEPC and cyNADP-ME activities related to malate catabolism have significant negative correlations with fruit quality. There is a positive correlation between organic acid content, firmness, and PEPC activity and indicators regulating malate metabolism. This demonstrates that the measured indicators in the study effectively prove the relationship between the organic acid concentration and their metabolism. The gene transcription levels that relate to malate metabolism are also positively correlated with the organic acid content, but the correlation levels were relatively lower. This may be because intracellular malate metabolism needs to be coordinated by multiple genes.

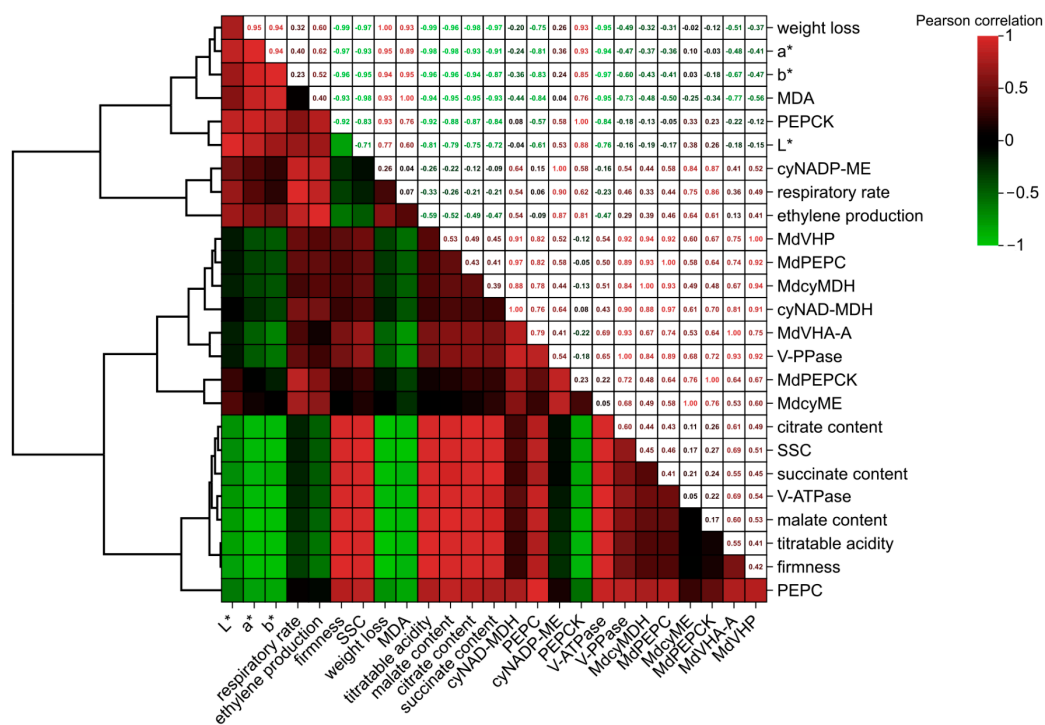


Figure 9. Pearson correlation analysis among the measured parameters.

4. Conclusions

The present study indicates that NFT storage can delay fruit senescence and suppress organic acid depletion. Storage at NFTs delayed the decrease in fruit firmness, maintained the SSC, reduced fruit weight loss, and inhibited MDA accumulation. Notably, compared to the control, NFT storage efficiently maintained fruit acidity, TA, and the malate content throughout storage. This was achieved through the upregulation of enzymes and the corresponding gene expression involved in malate biosynthesis as well as the malate transport-related enzymes and genes resulting in higher malate biosynthesis and accumulation. Moreover, the enzymes and corresponding genes involved in malate degradation were inhibited by storage at NFTs. Further research will study the shelf-life quality, other flavor substances, cell-membrane lipid profiles of fruit, and the energy cost of NFT storage.

Supplementary Materials: The following supporting information can be downloaded at: <https://www.mdpi.com/article/10.3390/agriculture14071057/s1>, Figure S1: Schematic diagram of near-freezing temperature storage machine; Figure S2: Schematic diagram of near-freezing temperature (NFT) storage equipment (A and B). The biological freezing curve of apple fruit (C) and the diagram of near-freezing temperature (D); Figure S3: The correlation between soluble solids and NFTs; Table S1: The NFTs applied over the storage period.

Author Contributions: Conceptualization, W.J. and C.S.; methodology, C.S.; software, C.S.; validation, C.S; formal analysis, C.S. and B.L.; investigation, C.S., B.L., H.Z., and K.C.; resources, W.J.; data curation, C.S. and W.J.; writing—original draft preparation, C.S.; writing—review and editing, C.S., B.L. and H.Z.; visualization, C.S.; supervision, W.J.; project administration, W.J.; funding acquisition, W.J. All authors have read and agreed to the published version of the manuscript.

Funding: This research was supported by the National Natural Science Foundation of China (No. 32172270).

Data Availability Statement: The data presented in this study are available on request from the corresponding author.

Conflicts of Interest: The authors declare no conflicts of interest.

References

1. Bondonno, N.P.; Bondonno, C.P.; Ward, N.C.; Hodgson, J.M.; Croft, K.D. The Cardiovascular Health Benefits of Apples: Whole Fruit vs. Isolated Compounds. *Trends Food Sci. Technol.* **2017**, *69*, 243–256. [[CrossRef](#)]
2. da Rocha Neto, A.C.; Beaudry, R.; Maraschin, M.; Di Piero, R.M.; Almenar, E. Double-Bottom Antimicrobial Packaging for Apple Shelf-Life Extension. *Food Chem.* **2019**, *279*, 379–388. [[CrossRef](#)] [[PubMed](#)]
3. Paul, V.; Pandey, R. Delaying Tomato Fruit Ripening by Using 1-Methylcyclopropene (1-MCP) for Better Postharvest Management: Current Status and Prospects in India. *Indian J. Plant Physiol.* **2013**, *18*, 195–207. [[CrossRef](#)]
4. Ma, Y.; Zhang, C.; Chen, G.; Jiang, W.; Cao, J. Controlled Freezing Storage (CFS) Maintains Quality of Fresh Edible Buds of Daylily (*Heemerocallis citrina*) by Enhancing Antioxidant Capacity, Energy Charge and Unsaturation of Fatty Acids. *Postharvest Biol. Technol.* **2024**, *213*, 112932. [[CrossRef](#)]
5. Jiang, H.; Hong, W.; Zhang, Y.; Liu, S.; Jiang, H.; Xia, S.; Si, X.; Li, B. Effects of Static Magnetic Field-Prolonged Supercooling Preservation on Blueberry Quality. *Food Biosci.* **2024**, *59*, 103771. [[CrossRef](#)]
6. Fan, X.; Xi, Y.; Zhao, H.; Liu, B.; Cao, J.; Jiang, W. Improving Fresh Apricot (*Prunus armeniaca* L.) Quality and Antioxidant Capacity by Storage at near Freezing Temperature. *Sci. Hortic.* **2018**, *231*, 1–10. [[CrossRef](#)]
7. Qin, J.; Chen, X.; Tang, X.; Shao, X.; Lai, D.; Xiao, W.; Zhuang, Q.; Wang, W.; Dong, T. Near-Freezing Temperature Suppresses Avocado (*Persea americana* Mill.) Fruit Softening and Chilling Injury by Maintaining Cell Wall and Reactive Oxygen Species Metabolism during Storage. *Plant Physiol. Biochem.* **2024**, *210*, 108621. [[CrossRef](#)]
8. Xiao, J.; Gu, C.; Zhu, D.; Chao, H.; Liang, Y.; Quan, S. Near-Freezing Temperature (NFT) Storage Alleviates Chilling Injury by Enhancing Antioxidant Metabolism of Postharvest Guava (*Psidium guajava* L.). *Sci. Hortic.* **2022**, *305*, 111395. [[CrossRef](#)]
9. Zhao, H.; Jiao, W.; Cui, K.; Fan, X.; Shu, C.; Zhang, W.; Cao, J.; Jiang, W. Near-Freezing Temperature Storage Enhances Chilling Tolerance in Nectarine Fruit through Its Regulation of Soluble Sugars and Energy Metabolism. *Food Chem.* **2019**, *289*, 426–435. [[CrossRef](#)]
10. Zhao, H.; Liu, B.; Zhang, W.; Cao, J.; Jiang, W. Enhancement of Quality and Antioxidant Metabolism of Sweet Cherry Fruit by Near-Freezing Temperature Storage. *Postharvest Biol. Technol.* **2019**, *147*, 113–122. [[CrossRef](#)]
11. Elfalleh, W.; Guo, L.; He, S.; Wang, P.; Cui, J.; Ma, Y. Characteristics of Cell Wall Structure of Green Beans during Controlled Freezing Point Storage. *Int. J. Food Prop.* **2015**, *18*, 1756–1772. [[CrossRef](#)]
12. Etienne, A.; Génard, M.; Lobit, P.; Mbeguié-A-Mbégué, D.; Bugaud, C. What Controls Fleshy Fruit Acidity? A Review of Malate and Citrate Accumulation in Fruit Cells. *J. Exp. Bot.* **2013**, *64*, 1451–1469. [[CrossRef](#)]
13. Liu, B.; Jiao, W.; Wang, B.; Shen, J.; Zhao, H.; Jiang, W. Near Freezing Point Storage Compared with Conventional Low Temperature Storage on Apricot Fruit Flavor Quality (Volatile, Sugar, Organic Acid) Promotion during Storage and Related Shelf Life. *Sci. Hortic.* **2019**, *249*, 100–109. [[CrossRef](#)]
14. Kader, A.A. Flavor Quality of Fruits and Vegetables. *J. Sci. Food Agric.* **2008**, *88*, 1863–1868. [[CrossRef](#)]
15. Yun, Z.; Jin, S.; Ding, Y.; Wang, Z.; Gao, H.; Pan, Z.; Xu, J.; Cheng, Y.; Deng, X. Comparative Transcriptomics and Proteomics Analysis of Citrus Fruit, to Improve Understanding of the Effect of Low Temperature on Maintaining Fruit Quality during Lengthy Post-Harvest Storage. *J. Exp. Bot.* **2012**, *63*, 2873–2893. [[CrossRef](#)] [[PubMed](#)]
16. Kweon, H.J.; Kang, I.K.; Kim, M.J.; Lee, J.; Moon, Y.S.; Choi, C.; Choi, D.G.; Watkins, C.B. Fruit Maturity, Controlled Atmosphere Delays and Storage Temperature Affect Fruit Quality and Incidence of Storage Disorders of “Fuji” Apples. *Sci. Hortic.* **2013**, *157*, 60–64. [[CrossRef](#)]
17. Guo, L.X.; Shi, C.Y.; Liu, X.; Ning, D.Y.; Jing, L.F.; Yang, H.; Liu, Y.Z. Citrate Accumulation-Related Gene Expression and/or Enzyme Activity Analysis Combined with Metabolomics Provide a Novel Insight for an Orange Mutant. *Sci. Rep.* **2016**, *6*, 29343. [[CrossRef](#)] [[PubMed](#)]
18. Onik, J.C.; Xie, Y.; Duan, Y.; Hu, X.; Wang, Z.; Lin, Q. UV-C Treatment Promotes Quality of Early Ripening Apple Fruit by Regulating Malate Metabolizing Genes during Postharvest Storage. *PLoS ONE* **2019**, *14*, e0215472. [[CrossRef](#)]
19. Zhao, J.; Quan, P.; Liu, H.; Li, L.; Qi, S.; Zhang, M.; Zhang, B.; Li, H.; Zhao, Y.; Ma, B.; et al. Transcriptomic and Metabolic Analyses Provide New Insights into the Apple Fruit Quality Decline during Long-Term Cold Storage. *J. Agric. Food Chem.* **2020**, *68*, 4699–4716. [[CrossRef](#)]
20. Bai, Y.; Dougherty, L.; Cheng, L.; Xu, K. A Co-Expression Gene Network Associated with Developmental Regulation of Apple Fruit Acidity. *Mol. Genet. Genom.* **2015**, *290*, 1247–1263. [[CrossRef](#)]
21. Yao, Y.-X.; Li, M.; Zhai, H.; You, C.-X.; Hao, Y.-J. Isolation and Characterization of an Apple Cytosolic Malate Dehydrogenase Gene Reveal Its Function in Malate Synthesis. *J. Plant Physiol.* **2011**, *168*, 474–480. [[CrossRef](#)] [[PubMed](#)]
22. Yao, Y.-X.; Li, M.; Liu, Z.; You, C.-X.; Wang, D.-M.; Zhai, H.; Hao, Y.-J. Molecular Cloning of Three Malic Acid Related Genes MdPEPC, MdVHA-A, MdCYME and Their Expression Analysis in Apple Fruits. *Sci. Hortic.* **2009**, *122*, 404–408. [[CrossRef](#)]
23. Batista-Silva, W.; Nascimento, V.L.; Medeiros, D.B.; Nunes-Nesi, A.; Ribeiro, D.M.; Zsögön, A.; Araújo, W.L. Modifications in Organic Acid Profiles During Fruit Development and Ripening: Correlation or Causation? *Front. Plant Sci.* **2018**, *9*, 1689. [[CrossRef](#)] [[PubMed](#)]
24. Liu, R.; Wang, Y.; Qin, G.; Tian, S. Molecular Basis of 1-Methylcyclopropene Regulating Organic Acid Metabolism in Apple Fruit during Storage. *Postharvest Biol. Technol.* **2016**, *117*, 57–63. [[CrossRef](#)]
25. Han, S.; Nan, Y.; Qu, W.; He, Y.; Ban, Q.; Lv, Y.; Rao, J. Exogenous γ -Aminobutyric Acid Treatment That Contributes to Regulation of Malate Metabolism and Ethylene Synthesis in Apple Fruit during Storage. *J. Agric. Food Chem.* **2018**, *66*, 13473–13482. [[CrossRef](#)] [[PubMed](#)]

26. Fan, X.; Zhao, H.; Wang, X.; Cao, J.; Jiang, W. Sugar and Organic Acid Composition of Apricot and Their Contribution to Sensory Quality and Consumer Satisfaction. *Sci. Hortic.* **2017**, *225*, 553–560. [[CrossRef](#)]
27. Mikulic-Petkovsek, M.; Ivancic, A.; Schmitzer, V.; Veberic, R.; Stampar, F. Comparison of Major Taste Compounds and Antioxidative Properties of Fruits and Flowers of Different Sambucus Species and Interspecific Hybrids. *Food Chem.* **2016**, *200*, 134–140. [[CrossRef](#)] [[PubMed](#)]
28. Terrier, N.; Sauvage, F.X.; Ageorges, A.; Romieu, C. Changes in Acidity and in Proton Transport at the Tonoplast of Grape Berries during Development. *Planta* **2001**, *213*, 20–28. [[CrossRef](#)]
29. Merlo, L.; Ferretti, M.; Ghisi, R.; Passera, C. Developmental Changes of Enzymes of Malate Metabolism in Relation to Respiration, Photosynthesis and Nitrate Assimilation in Peach Leaves. *Physiol. Plant.* **1993**, *89*, 71–76. [[CrossRef](#)]
30. Walker, R.; Chen, Z.; Técsi, L.; Famiani, F.; Lea, P.; Leegood, R. Phosphoenolpyruvate Carboxykinase Plays a Role in Interactions of Carbon and Nitrogen Metabolism during Grape Seed Development. *Planta* **1999**, *210*, 9–18. [[CrossRef](#)]
31. Liu, H.; Liu, Y.; Yu, B.; Liu, Z.; Zhang, W. Increased Polyamines Conjugated to Tonoplast Vesicles Correlate with Maintenance of the H⁺-ATPase and H⁺-PPase Activities and Enhanced Osmotic Stress Tolerance in Wheat. *J. Plant Growth Regul.* **2004**, *23*, 156–165. [[CrossRef](#)]
32. Ohnishi, T.; Gall, R.S.; Mayer, M.L. An Improved Assay of Inorganic Phosphate in the Presence of Extralabile Phosphate Compounds: Application to the ATPase Assay in the Presence of Phosphocreatine. *Anal. Biochem.* **1975**, *69*, 261–267. [[CrossRef](#)] [[PubMed](#)]
33. Bradford, M.M. A Rapid and Sensitive Method for the Quantitation of Microgram Quantities of Protein Utilizing the Principle of Protein-Dye Binding. *Anal. Biochem.* **1976**, *72*, 248–254. [[CrossRef](#)] [[PubMed](#)]
34. Livak, K.J.; Schmittgen, T.D. Analysis of Relative Gene Expression Data Using Real-Time Quantitative PCR and the 2[−]ΔΔCT Method. *Methods* **2001**, *25*, 402–408. [[CrossRef](#)] [[PubMed](#)]
35. Mditshwa, A.; Fawole, O.A.; Opara, U.L. Recent Developments on Dynamic Controlled Atmosphere Storage of Apples—A Review. *Food Packag. Shelf Life* **2018**, *16*, 59–68. [[CrossRef](#)]
36. Gago, C.M.L.; Guerreiro, A.C.; Miguel, G.; Panagopoulos, T.; da Silva, M.M.; Antunes, M.D.C. Effect of Calcium Chloride and 1-MCP (SmartfreshTM) Postharvest Treatment on ‘Golden Delicious’ Apple Cold Storage Physiological Disorders. *Sci. Hortic.* **2016**, *211*, 440–448. [[CrossRef](#)]
37. Marin, A.B.; Colonna, A.E.; Kudo, K.; Kupferman, E.M.; Mattheis, J.P. Measuring Consumer Response to ‘Gala’ Apples Treated with 1-Methylcyclopropene (1-MCP). *Postharvest Biol. Technol.* **2009**, *51*, 73–79. [[CrossRef](#)]
38. Both, V.; Brackmann, A.; Thewes, F.R.; Weber, A.; Schultz, E.E.; Ludwig, V. The Influence of Temperature and 1-MCP on Quality Attributes of ‘Galaxy’ Apples Stored in Controlled Atmosphere and Dynamic Controlled Atmosphere. *Food Packag. Shelf Life* **2018**, *16*, 168–177. [[CrossRef](#)]
39. Douglas Goff, H. Low-Temperature Stability and the Glassy State in Frozen Foods. *Food Res. Int.* **1992**, *25*, 317–325. [[CrossRef](#)]
40. Teixeira, A.S.; Elena González-Benito, M.; Molina-García, A.D. Glassy State and Cryopreservation of Mint Shoot Tips. *Biotechnol. Prog.* **2013**, *29*, 707–717. [[CrossRef](#)]
41. Cárdenas-Pérez, S.; Chanona-Pérez, J.; Méndez-Méndez, J.V.; Calderón-Domínguez, G.; López-Santiago, R.; Perea-Flores, M.J.; Arzate-Vázquez, I. Evaluation of the Ripening Stages of Apple (Golden Delicious) by Means of Computer Vision System. *Biosyst. Eng.* **2017**, *159*, 46–58. [[CrossRef](#)]
42. Gwanpua, S.G.; Verlinden, B.E.; Hertog, M.L.A.T.M.; Nicolai, B.M.; Hendrickx, M.; Geeraerd, A. Slow Softening of Kanzi Apples (*Malus × domestica* L.) Is Associated with Preservation of Pectin Integrity in Middle Lamella. *Food Chem.* **2016**, *211*, 883–891. [[CrossRef](#)] [[PubMed](#)]
43. Li, Y.; Zhao, Y.; Zhang, Z.; He, H.; Shi, L.; Zhu, X.; Cui, K. Near-Freezing Temperature Storage Improves Shelf-Life and Suppresses Chilling Injury in Postharvest Apricot Fruit (*Prunus armeniaca* L.) by Regulating Cell Wall Metabolism. *Food Chem.* **2022**, *387*, 132921. [[CrossRef](#)] [[PubMed](#)]
44. Hoehn, E.; Gasser, F.; Guggenbühl, B.; Künsch, U. Efficacy of Instrumental Measurements for Determination of Minimum Requirements of Firmness, Soluble Solids, and Acidity of Several Apple Varieties in Comparison to Consumer Expectations. *Postharvest Biol. Technol.* **2003**, *27*, 27–37. [[CrossRef](#)]
45. Cohen, S.; Itkin, M.; Yeselson, Y.; Tzuri, G.; Portnoy, V.; Harel-Baja, R.; Lev, S.; Saà Ar, U.; Davidovitz-Rikanati, R.; Baranes, N.; et al. The PH Gene Determines Fruit Acidity and Contributes to the Evolution of Sweet Melons. *Nat. Commun.* **2014**, *5*, 4026. [[CrossRef](#)]
46. Sweetman, C.; Deluc, L.G.; Cramer, G.R.; Ford, C.M.; Soole, K.L. Regulation of Malate Metabolism in Grape Berry and Other Developing Fruits. *Phytochemistry* **2009**, *70*, 1329–1344. [[CrossRef](#)]
47. Zheng, L.; Ma, W.; Liu, P.; Song, S.; Wang, L.; Yang, W.; Ren, H.; Wei, X.; Zhu, L.; Peng, J.; et al. Transcriptional Factor MdESE3 Controls Fruit Acidity by Activating Genes Regulating Malic Acid Content in Apple. *Plant Physiol.* **2024**, kiae282. [[CrossRef](#)] [[PubMed](#)]

Disclaimer/Publisher’s Note: The statements, opinions and data contained in all publications are solely those of the individual author(s) and contributor(s) and not of MDPI and/or the editor(s). MDPI and/or the editor(s) disclaim responsibility for any injury to people or property resulting from any ideas, methods, instructions or products referred to in the content.